IEEE Access
Multidisciplinary ⋮ Rapid Review ⋮ Open Access Journal

Received February 14, 2020, accepted March 1, 2020, date of publication March 4, 2020, date of current version March 18, 2020.

Digital Object Identifier 10.1109/ACCESS.2020.2978301

A Robust Model-Based Approach for Bearing Remaining Useful Life Prognosis in Wind Turbines

WEI TENG[1], CHEN HAN[1], YANKANG HU[1], XIN CHENG[2], LEI SONG[3], AND YIBING LIU[1]

[1]Key Laboratory of Power Station Energy Transfer Conversion and System, Ministry of Education, North China Electric Power University, Beijing 102206, China
[2]School of Mechanical and Electronic Engineering, Wuhan University of Technology, Wuhan 430070, China
[3]Key Laboratory of Space Utilization, Technology and Engineering Center for Space Utilization, Chinese Academy of Sciences, Beijing 100094, China

Corresponding author: Xin Cheng (chengx@whut.edu.cn)

This work was supported in part by the National Natural Science Foundation of China under Grant 51775186 and Grant 51575411, in part by the Fundamental Research Funds for the Central Universities of China under Grant 2018MS013, and in part by the Open Research Fund of Key Laboratory of Space Utilization, Chinese Academy of Sciences, under Grant LSU-KFJJ-2019-09.

ABSTRACT Accurate remaining useful life prognosis of bearings in wind turbines can effectively help to schedule maintenance strategy and reduce operational costs at wind farms. Unscented particle filter is good at state tracking in nonlinear problem. A robust model-based approach based on improved unscented particle filter is presented to deal with bearing life prognosis in wind turbines, which involves: (1) The mean of sigma points after unscented Kalman transform is regarded as the particles in particle filter to guarantee the particles aggregation; (2) Several past measurements are utilized to estimate the likelihood function of current step; (3) Uniform distribution is adopted for resampling particles to make them diversity. The presented remaining useful life prognosis approach depends more on the measurement, rather than the initial parameters of degradation model, which makes it practicable for the on-site wind turbines. Three life-cycle bearings from wind turbine high-speed shafts demonstrate the effectiveness of the proposed approach.

INDEX TERMS Remaining useful life, prognosis, bearings, wind turbines, improved unscented particle filter.

I. INTRODUCTION

Wind energy has rapidly developed in the past decade worldwide. In China, by the end of 2018, over 221.6 GW of installed capacity of wind energy has been put into operation [1], contributing about 6% of the total power supply. Wind turbine is the key equipment converting stochastic wind energy into electric power. Rolling bearings are extensively equipped in wind turbine drivetrain to support the rotating parts. Due to harsh operational environment, bearings in wind turbines are subject to fail, causing long shutdown and high cost. A series of worse consequences could be generated by the failed bearings, *e. g.*, the scuffing of generator between stator and rotor, the damage of wind turbine gearbox.

On the basis of the current and former health states of rotating machinery, or the failure law of congeneric subassemblies, the technique of remaining useful life (RUL) prognosis enables tendency prediction of health indicator representing the deterioration process of faulty wind turbines, and computes the time when the predicted indicator will arrive at failure threshold. After incipient faults are detected, RUL prognosis can tell operators when the faulty subassembly will fail and how long the spare part should be prepared in advance. Therefore, accurate RUL prognosis is significant in scheduling maintenance plan and reducing operational cost at wind farms.

Numerous RUL prediction approaches can be categorized into three types according to their principles: data driven approach, model-based approach, and the combination of the above two methods [2]. Data driven prognosis first constructs multiple failure models on the basis of historical data. Through comparing the similarity between the online indicator and the historical models, the predicted machinery is assumed to comply with the failure law of the historical model with the largest similarity, and RUL can be calculated according to this model. Unfortunately, data driven approach needs

The associate editor coordinating the review of this manuscript and approving it for publication was Chandan Kumar.

This work is licensed under a Creative Commons Attribution 4.0 License. For more information, see https://creativecommons.org/licenses/by/4.0/

abundant historical life-cycle data that is hardly acquired in industrial applications. Moreover, the assumption of the predicted machinery complying with the failure law of the historical model with the largest similarity is not rigorous because congeneric machineries may work under different operational conditions. Model-based approach assumes the failure process obeying some physical law with a specific mathematic formula, *e. g*., fatigue cracks complying with Paris-Erdogan model [3], fatigue of coil spring with Goodman formula [4], and laser device with inverse Gaussian degradation model [5].

Particle filter is a model-based algorithm widely applied in object tracking under non-Gaussian and nonlinear conditions [6]–[8]. Compared with Kalman filter [9] and its variants, particle filter has a better performance for dealing with non-Gaussian and nonlinear problems. Because of these properties, particle filter has been utilized in the RUL prediction of various devices. Lei *et al*. [10] used the maximum-likelihood estimation to initialise model parameters and particle filter to predict the RUL of bearings. Zio and Peloni [11] proposed a methodology for the estimation of the remaining useful life of component based on particle filter. Chen *et al*. [12] proposed a machine remaining useful life prediction approach based on adaptive neuro-fuzzy inference systems and high order particle filter. Fan *et al*. [13] made an approach on long-term lumen maintenance life prediction based on particle filter. Raghavana and Frey [14] used particle filter to predict lifetime of microelectronic devices. Orchard and Vachtsevanos [15] proposed a particle filtering-based framework for real-time fault diagnosis and failure prognosis in turbine engine. Deutsch *et al.* [27] integrated deep belief network and particle filter for RUL prediction of hybrid ceramic bearings. For the application of RUL prediction in wind turbine systems, Cheng *et al.* developed enhanced particle filtering algorithm [28] to predict the remaining useful life of a bearing in a 2.5 MW wind turbine. They also defined noise-to-signal ratio as the fault-related feature for fault prognosis, and used adaptive neuro-fuzzy inference system and particle filtering to predict the RUL of wind turbine gearbox [29]. Djeziri *et al.* [30] proposed a hybrid method of a wind turbine fault prognosis, involving a physical model, cluster and geolocation principle.

Unscented particle filter (UPF) combines unscented Kalman transform and particle filter to deal with nonlinear tracking problem [16]. Unscented Kalman transform enables the nonlinear transfer of the mean and variance of particles, which generates proposal distributions that match the true posterior closely. With these advantages, Acuña and Orchard [17] proposed a particle filter based failure prognosis via sigma points application to lithium-Ion battery state-of-charge monitoring. Zheng and Fang [18] integrated unscented Kalman filter and relevance vector regression for the lithium-ion battery remaining useful life and short-term capacity prediction. Another significant work in RUL prognosis is the construction of health indicator. A quantitative degradation assessment of bearings was fulfilled by calculation of minimum quantization error of the new measurement data to a trained Self Organizing Map (SOM) neural network using normal operation data sets [19]. The combination of SOM and other methods were developed for health trend prediction of rotating bearings [20], [21]. For the bearings RUL prognosis in wind turbines, Teng *et al*. [22] selected root mean square and frequency spectrum energy as health indicators. Guo *et al*. [23] adopted recurrent neural network with feature selection technique to build the health indicator.

In this paper, a robust model-based approach on the basis of improved unscented particle filter is presented to predict the remaining useful life of bearings in wind turbines. Three key points are involved: (1) The mean of the particles in unscented Kalman transform is used as the particles in particle filter, making a favorable particles aggregation; (2) The past several measurements are utilized to calculate the likelihood function of current step; (3) To overcome the particle unicity, a modified resampling method using uniform distribution is presented. The presented approach depends more on the measurements rather than the initial parameters, and has no requirement for the complex construction technique of health indicators. Three life-cycle bearings from on-site wind turbine high-speed shafts verify the effectiveness of the approach.

II. UNSCENTED PARTICLE FILTER

A. PARTICLE FILTER

Particle filter is an extension of Kalman filter to realize nonlinear tracking. It no longer assumes the state or noise distribution obeying the Gaussian case [6]. A dynamic nonlinear system can be described as the state space (1) and (2)

$$\boldsymbol{x}_k = f(\boldsymbol{x}_{k-1}, \boldsymbol{v}_{k-1}) \tag{1}$$

$$\boldsymbol{z}_k = h(\boldsymbol{x}_k, \boldsymbol{\upsilon}_k) \tag{2}$$

where Eq. (1) is state model and Eq. (2) is measurement model. $\boldsymbol{x}_k$ and $\boldsymbol{z}_k$ are system state and measurement at thek^{th} step. f and h are state and measurement function. $\boldsymbol{v}_{k-1}$is state noise at the $(k\text{-}1)^{\text{th}}$ step and υ_k is measurement noise at the k^{th}step.

The aim of particle filter is to get the posterior density distribution $p(\boldsymbol{x}_{0:k}|\boldsymbol{z}_{1:k})$ through the known measurements $\boldsymbol{z}_{1:k}$. To get a recursive expression, $p(\boldsymbol{x}_{0:k}|\boldsymbol{z}_{1:k})$ is first analyzed. Theoretically, if enough particles obeying $p(\boldsymbol{x}_{0:k}|\boldsymbol{z}_{1:k})$ can be drawn, with reasonable weights $\boldsymbol{w}_k$, $p(\boldsymbol{x}_{0:k}|\boldsymbol{z}_{1:k})$ could be approximated as

$$p(\boldsymbol{x}_{0:k}|\boldsymbol{z}_{1:k}) \approx \sum_{i=1}^{N_s} \boldsymbol{w}_k^{(i)} \delta(\boldsymbol{x}_{0:k} - \boldsymbol{x}_{0:k}^{(i)}) \tag{3}$$

where N_s is the number of particles, $\boldsymbol{w}_k^{(i)}$ is the weight of the i^{th} particle, and $\boldsymbol{x}_{0:k}^{(i)}$ is the particle state from initial to the k^{th} step. In fact, the $p(\boldsymbol{x}_{0:k}|\boldsymbol{z}_{0:k})$ is unknown, thus a proposal density function $q(\boldsymbol{x}_{0:k}|\boldsymbol{z}_{0:k})$ is used to sample the numerous

particles. Then, the weight $\boldsymbol{w}_k^{(i)}$ has the following relationship:

$$\boldsymbol{w}_k^{(i)} \propto \frac{p(\boldsymbol{x}_{0:k}^{(i)}|z_{1:k})}{q(\boldsymbol{x}_{0:k}^{(i)}|z_{1:k})} \tag{4}$$

$q(\boldsymbol{x}_{0:k}|z_{1:k})$ is called importance density and it can be factorized as

$$q(\boldsymbol{x}_{0:k}|z_{1:k}) = q(\boldsymbol{x}_k|\boldsymbol{x}_{0:k-1}, z_{1:k})q(\boldsymbol{x}_{0:k-1}|z_{1:k-1}) \tag{5}$$

here $q(\boldsymbol{x}_{0:k-1}|z_{1:k-1})$ equals to $q(\boldsymbol{x}_{0:k-1}|z_{1:k})$ considering the concrete physical meaning. Then,

$$\begin{aligned} &p(\boldsymbol{x}_{0:k}|z_{1:k}) \\ &= \frac{p(z_k|\boldsymbol{x}_{0:k}, z_{1:k-1})p(\boldsymbol{x}_{0:k}|z_{1:k-1})}{p(z_k|z_{1:k-1})} \\ &= \frac{p(z_k|\boldsymbol{x}_{0:k}, z_{1:k-1})p(\boldsymbol{x}_k|\boldsymbol{x}_{0:k-1}, z_{1:k-1})}{p(z_k|z_{1:k-1})}p(\boldsymbol{x}_{0:k-1}|z_{1:k-1}) \\ &= \frac{p(z_k|\boldsymbol{x}_k)p(\boldsymbol{x}_k|\boldsymbol{x}_{k-1})}{p(z_k|z_{1:k-1})}p(\boldsymbol{x}_{0:k-1}|z_{1:k-1}) \\ &\propto p(z_k|\boldsymbol{x}_k)p(\boldsymbol{x}_k|\boldsymbol{x}_{k-1})p(\boldsymbol{x}_{0:k-1}|z_{1:k-1}) \end{aligned} \tag{6}$$

where $p(z_k|z_{1:k-1})$ denotes the correlation between the current measurement and previous ones. Since the measurements can be measured, their correlation is explicit and can be modelled by time series methods, so $p(z_k|z_{1:k-1})$ is regarded as a normalizing constant. Then sample some particles and substitute Eq. (5) and (6) into Eq. (4), the weight $\boldsymbol{w}_k^{(i)}$ can be updated as

$$\boldsymbol{w}_k^{(i)} = \boldsymbol{w}_{k-1}^{(i)} \frac{p(z_k|\boldsymbol{x}_k^{(i)})p(\boldsymbol{x}_k^{(i)}|\boldsymbol{x}_{k-1}^{(i)})}{q(\boldsymbol{x}_k^{(i)}|\boldsymbol{x}_{0:k-1}^{(i)}, z_{1:k})} \tag{7}$$

In common case, $q(\boldsymbol{x}_k^{(i)}|\boldsymbol{x}_{0:k-1}^{(i)}, z_{1:k})$ is replaced by $q(\boldsymbol{x}_k^{(i)}|\boldsymbol{x}_{k-1}^{(i)}, z_k)$ because $p(\boldsymbol{x}_k|z_{1:k})$ is recursively required at each step. So $\boldsymbol{w}_k^{(i)}$ is rewritten as

$$\boldsymbol{w}_k^{(i)} \propto \boldsymbol{w}_{k-1}^{(i)} \frac{p(z_k|\boldsymbol{x}_k^{(i)})p(\boldsymbol{x}_k^{(i)}|\boldsymbol{x}_{k-1}^{(i)})}{q(\boldsymbol{x}_k^{(i)}|\boldsymbol{x}_{k-1}^{(i)}, z_k)} \tag{8}$$

If the importance density $q(\boldsymbol{x}_k^{(i)}|\boldsymbol{x}_{k-1}^{(i)}, z_k)$ is chosen as $p(\boldsymbol{x}_k^{(i)}|\boldsymbol{x}_{k-1}^{(i)})$ [6] considering the computational cost, $\boldsymbol{w}_k^{(i)}$ is simplified as

$$\boldsymbol{w}_k^{(i)} \propto \boldsymbol{w}_{k-1}^{(i)} p(z_k|\boldsymbol{x}_k^{(i)}) \tag{9}$$

The above filtering procedure is named as sequential importance sampling (SIS) Filter. The posterior density $p(\boldsymbol{x}_k|z_{1:k})$ is estimated as

$$p(\boldsymbol{x}_k|z_{1:k}) \approx \sum_{i=1}^{N_s} \boldsymbol{w}_k^{(i)} \delta(\boldsymbol{x}_k - \boldsymbol{x}_k^{(i)}) \tag{10}$$

B. UNSCENTED PARTICLE FILTER

Unscented particle filter (UPF) consists of an unscented Kalman filter and a particle filter. In unscented Kalman transform, each particle with the sigma points at the $(k\text{-}1)^{\text{th}}$ step is processed by nonlinear state model and measurement model, which provides the estimation of proposal density function at the k^{th} step. Due to the introduction of new arrival measurement in unscented Kalman transform, the estimation of proposal density function approximates well to the posterior probability density.

For any particle vector $\boldsymbol{x}_{k-1}^{(i)a} = [\boldsymbol{x}_{k-1}^{(i)T}\ \boldsymbol{v}_{k-1}^{(i)T}\boldsymbol{\upsilon}_{k-1}^{(i)T}]^T$ consisting of particle state, state noise and measurement noise at the $(k\text{-}1)^{\text{th}}$ step, the sigma points are calculated as [16]

$$\boldsymbol{X}_{k-1}^{(i)a} = [\bar{\boldsymbol{x}}_{k-1}^{(i)a}\ \bar{\boldsymbol{x}}_{k-1}^{(i)a} \pm \sqrt{(n_a + \lambda)\mathbf{P}_{k-1}^{(i)a}}] \tag{11}$$

where $\bar{\boldsymbol{x}}_{k-1}^{(i)a}$ is the mean of the particle vectors, $\mathbf{P}_{k-1}^{(i)a}$ is the covariance of the particle vectors. $\boldsymbol{X}_{k-1}^{(i)a} = [(\boldsymbol{X}_{k-1}^{(i)x})^T\ (\boldsymbol{X}_{k-1}^{(i)v})^T(\boldsymbol{X}_{k-1}^{(i)\upsilon})^T]^T$, λ is composite scaling parameter. n_a is the dimension of particle vector, which is the sum of the dimension of particle state, state noise and measurement noise, $n_a = n_x + n_v + n_\upsilon$. There are $2n_a + 1$ sigma points for each particle.

The time updating process is as following:

$$\begin{aligned} \boldsymbol{X}_{k|k-1}^{(i)x} &= f(\boldsymbol{X}_{k-1}^{(i)x}, \boldsymbol{X}_{k-1}^{(i)v}) \\ \bar{\boldsymbol{x}}_{k|k-1}^{(i)} &= \sum_{j=0}^{2n_a} W_j^{(m)} \boldsymbol{X}_{j,k|k-1}^{(i)x} \\ \mathbf{P}_{k|k-1}^{(i)} &= \sum_{j=0}^{2n_a} W_j^{(c)} [\boldsymbol{X}_{j,k|k-1}^{(i)x} - \bar{\boldsymbol{x}}_{k|k-1}^{(i)}][\boldsymbol{X}_{j,k|k-1}^{(i)x} - \bar{\boldsymbol{x}}_{k|k-1}^{(i)}]^T \\ \mathbf{Z}_{k|k-1}^{(i)} &= h(\boldsymbol{X}_{k|k-1}^{(i)x}, \boldsymbol{X}_{k-1}^{(i)\upsilon}) \\ \bar{\boldsymbol{z}}_{k|k-1}^{(i)} &= \sum_{j=0}^{2n_a} W_j^{(m)} \boldsymbol{Z}_{j,k|k-1}^{(i)} \end{aligned} \tag{12}$$

Measurement update equations are:

$$\begin{aligned} \mathbf{P}_{\tilde{z}_k\tilde{z}_k} &= \sum_{j=0}^{2n_a} W_j^{(c)} [\boldsymbol{Z}_{j,k|k-1}^{(i)} - \bar{\boldsymbol{z}}_{k|k-1}^{(i)}][\boldsymbol{Z}_{j,k|k-1}^{(i)} - \bar{\boldsymbol{z}}_{k|k-1}^{(i)}]^T \\ \mathbf{P}_{x_k z_k} &= \sum_{j=0}^{2n_a} W_j^{(c)} [\boldsymbol{X}_{j,k|k-1}^{(i)} - \bar{\boldsymbol{x}}_{k|k-1}^{(i)}][\boldsymbol{Z}_{j,k|k-1}^{(i)} - \bar{\boldsymbol{z}}_{k|k-1}^{(i)}]^T \\ \mathbf{K}_k &= \mathbf{P}_{x_k z_k} \mathbf{P}_{\tilde{z}_k\tilde{z}_k}^{-1} \\ \bar{\boldsymbol{x}}_k^{(i)} &= \bar{\boldsymbol{x}}_{k|k-1}^{(i)} + \mathbf{K}_k(z_k - \bar{\boldsymbol{z}}_{k|k-1}^{(i)}) \\ \mathbf{P}_k^{(i)} &= \mathbf{P}_{k|k-1}^{(i)} - \mathbf{K}_k \mathbf{P}_{\tilde{z}_k\tilde{z}_k} \mathbf{K}_k^T \end{aligned} \tag{13}$$

$\mathbf{K}_k$ is Kalman gain, the weights of sigma points are computed as:

$$\begin{aligned} W_0^{(m)} &= \lambda/(n_a + \lambda) \\ W_0^{(c)} &= \lambda/(n_a + \lambda) + (1 - \alpha^2 + \beta) \\ W_j^{(m)} &= W_j^{(c)} = 1/\{2(n_a + \lambda)\}, \quad j = 1, 2, \ldots, 2n_a \end{aligned} \tag{14}$$

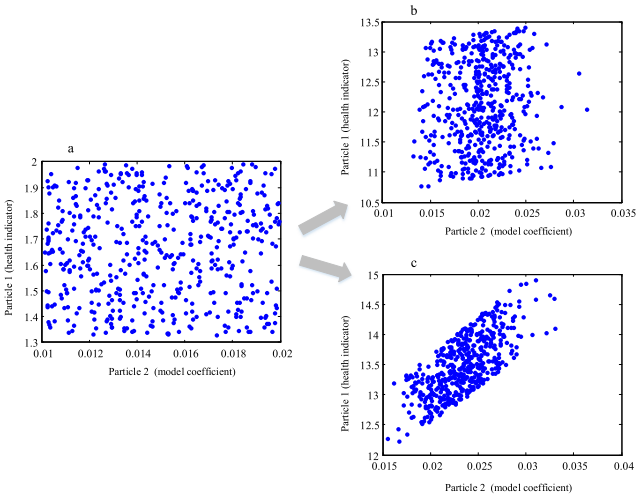

FIGURE 1. Comparison of particle distribution: a) initial particles; b) particle distribution of conventional particle filter; c) particle distribution using replacement method.

The proposal density function is estimated as $q(\boldsymbol{x}_k^{(i)}|\boldsymbol{x}_{k-1}^{(i)}, z_k) = \mathcal{N}(\bar{\boldsymbol{x}}_k^{(i)}, \mathbf{P}_k^{(i)})$. New particles are randomly drawn from this proposal function, and the transition prior $p(\boldsymbol{x}_k^{(i)}|\boldsymbol{x}_{k-1}^{(i)})$ and the likelihood $p(z_k|\boldsymbol{x}_k^{(i)})$ are calculated. The weights of particles are updated as Eq. (8).

III. IMPROVED UPF FOR BEARINGS RUL PROGNOSIS IN WIND TURBINE

A. IMPROVED UNSCENTED PARTICLE FILTER

Three improvements are implemented in this Section to make UPF practical for bearings RUL prognosis in wind turbines.

1) REPLACING PARTICLES BY THE MEAN IN UNSCENTED KALMAN TRANSFORM

Unscented Kalman transform in Eq. (12) absorbs the information of both state and measurement model. Since it is under the framework of particle filter, numerous of particles already exist, which enables to guarantee the particle diversity. Thus, to reduce the uncertainty of random samples from the estimated proposal density $q(\boldsymbol{x}_k^{(i)}|\boldsymbol{x}_{k-1}^{(i)}, z_k)$, only the unscented transformed mean $\bar{\boldsymbol{x}}_k^{(i)}$is utilized as new particle at the k^{th}step. The conventional SIS particle filter is still adopted in the RUL prediction with $\boldsymbol{x}_k^{(i)}$ replaced by $\bar{\boldsymbol{x}}_k^{(i)}$, and the weight Eq. (9) is rewritten as

$$\boldsymbol{w}_k^{(i)} \propto \boldsymbol{w}_{k-1}^{(i)} p(z_k|\bar{\boldsymbol{x}}_k^{(i)}) \tag{15}$$

Fig. 1 shows the comparison of particle distribution during one RUL prediction between conventional particle filter and replacement method. The two methods use the same initial particles shown in Fig. 1a. At the end of the RUL prediction, in Fig. 1c the particle distribution through replacing particles by the mean in unscented Kalman transform, shows preferable concentration than the distribution using conventional particle filter in Fig. 1b.

FIGURE 2. Stratified resampling.

2) LIKELIHOOD CALCULATION

In Eq. (15), to update the weights, the density function $p(z_k|\bar{\boldsymbol{x}}_k^{(i)})$ should be given or could be measured. However in RUL prognosis, only the measurement z_k at each step is measured, and the relationship between $\boldsymbol{x}_k$ and z_k in Eq. (2) is unknown. Here, to fully consider the effect of measurements, $p(z_k|\bar{\boldsymbol{x}}_k^{(i)})$ is approximated as

$$p(z_k|\bar{\boldsymbol{x}}_k^{(i)}) \sim \mathcal{N}\left(\text{abs}(z_k - \bar{\boldsymbol{x}}_k^{(i)}), \sigma^2(z_{k-N:\,k})\right) \tag{16}$$

where $\mathcal{N}$ denotes normal distribution, $\sigma^2(z_{k-N:\,k})$denotes the variance of the measurements from the $(k\text{-}N)^{\text{th}}$to k^{th} step, and N is the number of previous steps used for the estimation of the probability density function $p(z_k|\bar{\boldsymbol{x}}_k^{(i)})$.

3) IMPROVED RESAMPLING TECHNIQUE

Particle degeneracy is an inevitable phenomenon in particle filter due to the iterative calculation of particle weights. To overcome this, some resampling methods are applied to resample the particles during iterative calculation, including multinomial resampling, residual resampling and stratified resampling [24] *etc*. Considering its uniformity and randomicity, stratified resampling is adopted in this paper. As show in Fig. 2, the cumulative sum of the current weights is divided into N_s equal sections, and one particle is randomly selected from each section. This guarantees that each particle is between 0 and $2/N_s$ apart.

The effective sample size N_{eff} is computed to decide whether the resampling is triggered. $N_{eff}$is approximated as [6]

$$N_{eff} \approx 1/\sum_{i=1}^{N_s} \boldsymbol{w}_k^{(i)} \tag{17}$$

If $N_{eff} < N_s/2$, the stratified resampling is triggered.

To avoid the homogenization of resampled particles from stratified resampling, (that is, the particles with larger weights may be sampled multiple times), a further resampling algorithm is proposed, which will guarantee the diversity of resampled particles. The improved resampling algorithm is shown in Table 1.

where ind(i) is resampled particle indices from stratified resampling, $\mathcal{U}$ denotes uniform distribution.

With the updated particles and weights at the k^{th} step, the current particle state is estimated as

$$\hat{\boldsymbol{x}}_k \approx \sum_{i=1}^{N_s} \boldsymbol{w}_k^{(i)} \bar{\boldsymbol{x}}_k^{(i)} \tag{18}$$

The core of the improved resampling technique is the particle update after stratified resampling. Uniform distribution is used here can remain the particle states as normal distribution,

TABLE 1. Improved resampling algorithm.

If $N_{eff} < N_s/2$

Trigger stratified resampling

Indices with larger weights are obtained

For i=1:N_s

Update the state particles $\bar{\boldsymbol{x}}_k^{(i)} \sim \mathcal{U}\left(0.9\bar{\boldsymbol{x}}_k(\text{ind}(i)), 1.1\bar{\boldsymbol{x}}_k(\text{ind}(i))\right)$

Update weights $\boldsymbol{w}_k^{(i)} \sim \mathcal{U}\left(0.9\boldsymbol{w}_k(\text{ind}(i)), 1.1\boldsymbol{w}_k(\text{ind}(i))\right)$

end

end

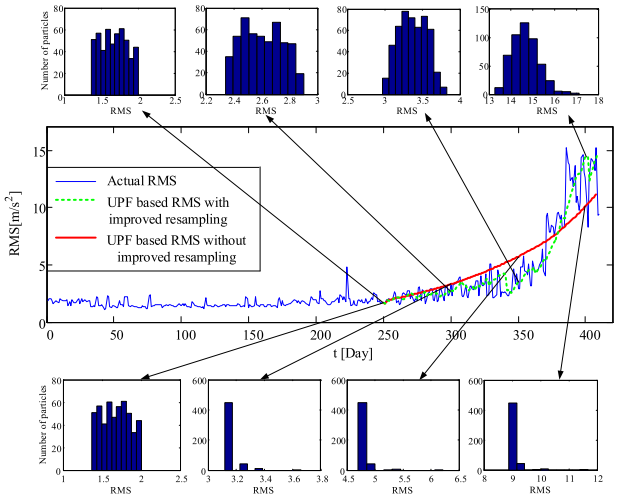

FIGURE 3. Particle distribution of health state at different times.

meanwhile enhancing the diversity of particles by the random coefficient between 0.9 and 1.1 in Table 1.

In Fig. 3, due to the improved resampling technique, the top sub-figures always exhibits approximate normal distribution and particle diversity at different times. By contrast, even the same initial particles, the particles degenerate severely in the bottom-right sub-figures without the improved resampling method.

B. BEARINGS RUL PROGNOSIS BASED ON IMPROVED UPF

Rolling bearings are widely utilized in industrial equipment to support rotating machineries. The life-cycle of rolling bearings can be divided into several phases: health stage, incipient fault, deteriorating stage and failure stage. The degradation process of rolling bearings is depicted as an exponential model that is shown as

$$\begin{cases} x_k = \exp(b_k \cdot k) \cdot x_{k-1} \\ z_k = x_k + \sigma_z \end{cases} \tag{19}$$

where x_{k-1} is the bearing state at the (k-1)$^{\text{th}}$ step, b_k is the model coefficient, $z_k$is the measurement, which can be the health indicator of rolling bearing. σ_z denotes the standard deviation of measurement noise.

TABLE 2. The proposed RUL prognosis procedure for bearings using improved UPF.

Model definition, Eq. (19);

Detect the incipient fault and determine the RUL prediction time

k=1;

Sample initial particles $b_1^{(i)} \sim \mathcal{U}(m, n),\ i = 1, 2, \cdots, N_s$;

Sample initial particles $x_1^{(i)} \sim \mathcal{U}\left(0.9z_1, 1.1z_1\right),\ i = 1, 2, \cdots, N_s$;

Implement UPF for each particles using Eqs. (12) (13);

Calculate the likelihood function, Eq. (16);

Update the weights, Eq. (15);

Implement the resampling algorithm in Table I,

$\bar{\boldsymbol{x}}_k^{(i)} = [\bar{x}_k^{(i)}, b_k^{(i)}]^T$;

Update the particles in Eq. (18);

Compute the future state until touching the threshold, and

obtain the RUL at the current step, Eq. (20);

k=k+1;

Repeat

The difficulty of predicting the remaining useful life of bearings lies in how to determine the model coefficient b_k. The common usage is to preset b in an initial range $[m, n]$ and to update it using the arriving measurements. The initial range of parameter b is determined as follows: (1) When RMS increases, it denotes incipient tendency. At that stage, the local maxima and minima of RMS are detected. With these points, the upper curve and lower curve are separately fitted by exponential function. Each curve generates a parameter b, thus forming a range. (2) Several bearings on the high-speed shafts are repeated as the last step. The minimal b from all the lower curves is set as the left boundary of the initial range, and the maximal b from all the upper curves is set as the right boundary. Thus, the particles $\boldsymbol{x}$ in bearing RUL prognosis are the ensemble of bearing state x and model coefficient b, $\boldsymbol{x} = [x,\ b]^{\text{T}}$. The bearings RUL prognosis procedure based on improved UPF is shown in Table 2.

At any step k, when the particle states including $\hat{x}_k$ and $\hat{b}_k$ are estimated as Eq. (18), the future state should be computed as the degradation model in Eq. (19) iteratively until it touches the failure threshold. Provided that the time touching the threshold is denoted by $\hat{t}_{kf}$, then the RUL at current step k is computed as

$$RUL_k = \hat{t}_{kf} - k \tag{20}$$

IV. CASE STUDY

A. THREE FAILURE BEARINGS IN WIND TURBINES

A typical drive train of wind turbines is shown in Fig. 4, which consists of blade, hub rotor, gearbox, and generator. From the hub rotor to the generator, the rotational speed

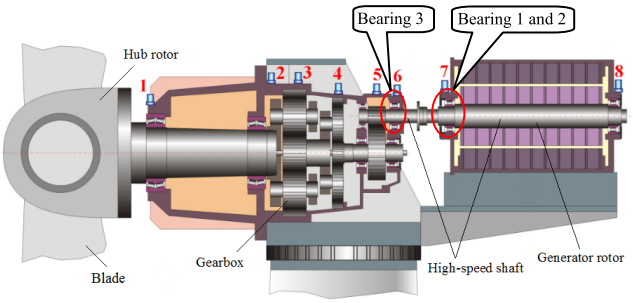

FIGURE 4. The drive train of wind turbines and the placement of accelerometers.

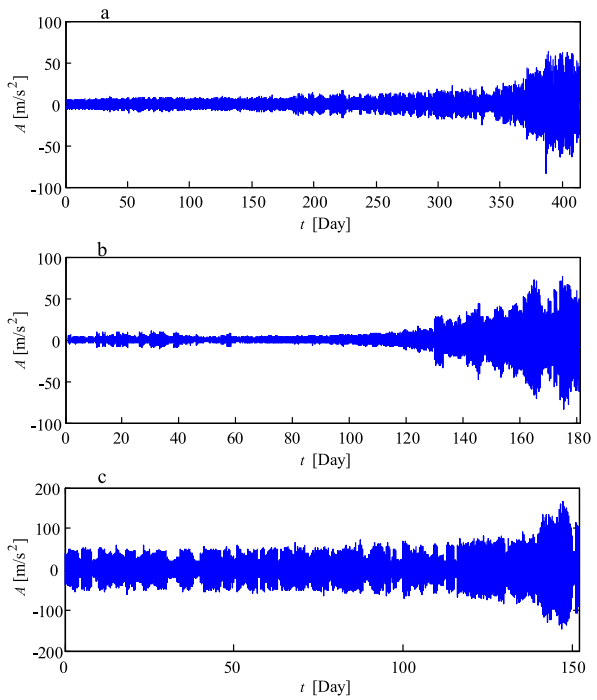

FIGURE 5. Life-cycle vibration signals from three wind turbines: a) bearing 1 from drive end of generator; b) bearing 2 from drive end of generator; c) bearing 3 from the rear end of high speed shaft in gearbox.

increases gradually. The last shaft in gearbox combined with the generator rotor are named as high-speed shaft. Generally, eight accelerometers are mounted on the surface of the drive train to monitor the health state of gears or bearings. In this paper, we focus on the bearings in wind turbine with high rotational speeds since abundant on-site cases exhibit that their degradation processes obey the exponential model as Eq. (19).

Fig. 5 displays the vibration signals of three life-cycle bearings from wind turbine high-speed shaft. The first two are from drive end of generator (accelerometer 7 in Fig. 4), and the last one is from the rear bearing on high speed shaft in wind turbine gearbox (accelerometer 6 in Fig. 4). The three bearings failed at the last day shown in Fig. 5. To avoid the disadvantages of varying operating conditions, only the vibration signals with the rotational speed over 1000 rpm of the generator were collected each day. The duration of each signal is 2 second. The sampling frequency of the first two bearings is 8192 Hz, and the last one is 51200 Hz as different data acquisition systems were utilized. Suffering from the fluctuating load from stochastic wind, the vibration amplitudes change obviously, but show evident tendency when severe faults emerge on the bearings. The first two failed bearings in generators are SKF 6326C3 and the third one in gearbox is FAG 31326, whose fault features are listed in Table 3. f_r is the rotating frequency of the generator shaft. Once the fault feature frequencies in Table 3 emerge continuously in power spectrum of vibration signal, the bearing could be deduced as incipient fault.

TABLE 3. Fault features of bearings in wind turbine generators.

	Ratio to f_r		
	Bearing 1	Bearing 2	Bearing 3
Cage	0.392	0.392	0.420
Rolling elements	2.20	2.20	2.694
Outer race	3.130	3.130	6.732
Inner race	4.870	4.870	9.240
Failure position	Inner and outer race	Outer race	Inner race

Taking bearing 1 for an example, the temporal signal, power spectrum and envelope spectrum at different health stages are shown in Fig. 6. At the 18th day in Fig. 6a, the vibration amplitude is limited into ± 10 m/s^2, and there are regular periodic fluctuations in the temporal signal. The fluctuating component corresponds to the rotating frequency, 29 Hz, of the generator. At this stage, the rotating frequency indicates a potential rotor imbalance, rather than bearing fault. At the 195th day in Fig. 6b, besides the rotating frequency ($f_r = 28$ Hz), the frequencies 87 Hz (3.1 times of f_r), 134 Hz (4.78 times of f_r) emerge, denoting the fault on outer race and inner race of the bearing. In Fig. 6c, the 370th day, the vibration amplitude continues to increase with the rotating frequency 30 Hz, the outer race fault frequency 93 Hz, and the inner race fault frequency 142 Hz. That shows the performance degradation of the bearing. At the 405th day in Fig. 6d, the bearing enters into the failure stage where the vibration amplitudes increase obviously, still accompanied by the fault frequencies of outer race, inner race and their harmonics in the envelope spectrum. Therefore, bearing 1 fails due to the fault on both inner and outer race. Similarly, from the analysis of envelope spectrum of bearing 2 and bearing 3, the failure positions are focused on outer race and inner race respectively, described in Table 3.

B. HEALTH INDICATOR AND FAILURE THRESHOLD

To develop a practical RUL prediction model for the on-site bearings on wind turbine high-speed shafts, simple and

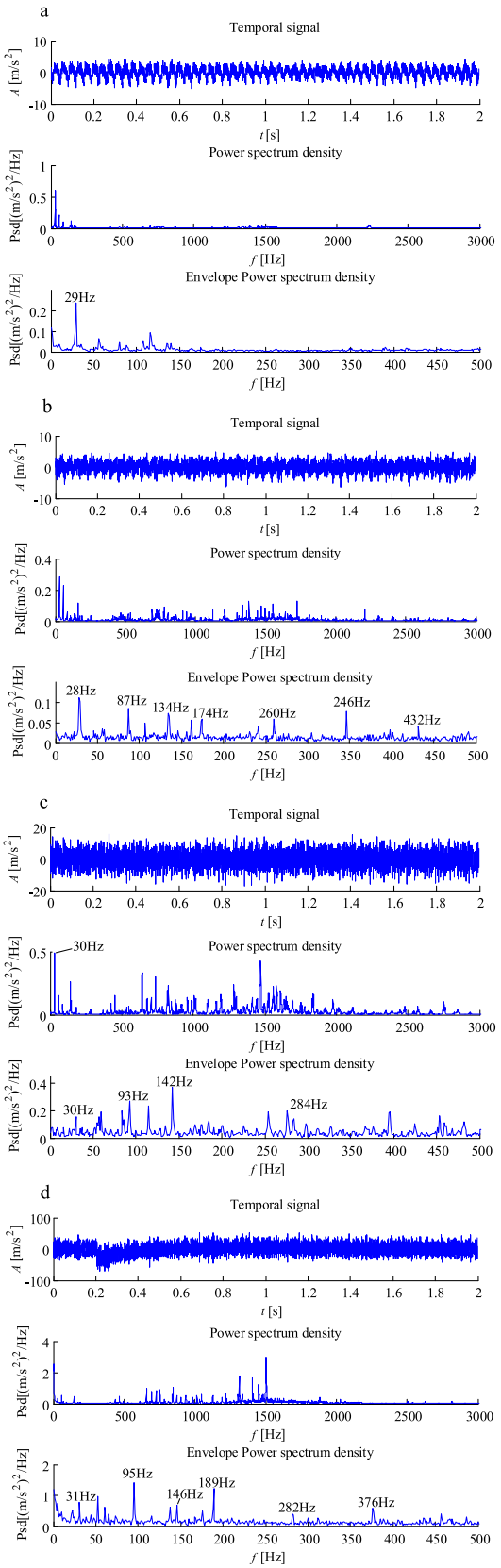

FIGURE 6. The temporal signal, power spectrum and envelope spectrum at different times of bearing 1: a) the 18th day; b) the 195th day; c) the 370th day; d) the 405th day.

TABLE 4. The statistical indicators of vibration signals.

Indicators	Formulas
Mean	$\bar{x} = \sum_{i=1}^{N} x_i / N$
Root mean square (RMS)	$x_{rms} = \sqrt{\sum_{i=1}^{N} x_i^2 / N}$
Variance	$x_v = \sum_{i=1}^{N} (x_i - \bar{x})^2 / N$
Square root of amplitude (SRA)	$x_{sra} = \left(\sum_{i=1}^{N} \sqrt{\lvert x_i \rvert} / N \right)^2$
Skewness	$x_{skew} = \sum_{i=1}^{N} (x_i - \bar{x})^3 / (N \cdot x_\sigma^3)$
Kurtosis	$x_{kurt} = \sum_{i=1}^{N} (x_i - \bar{x})^4 / (N \cdot x_\sigma^4)$
Waveform factor (WF)	$x_w = x_{rms} / \bar{x}$
Margin factor (MF)	$x_m = x_{max} / x_r$

where N is the data length of each section.

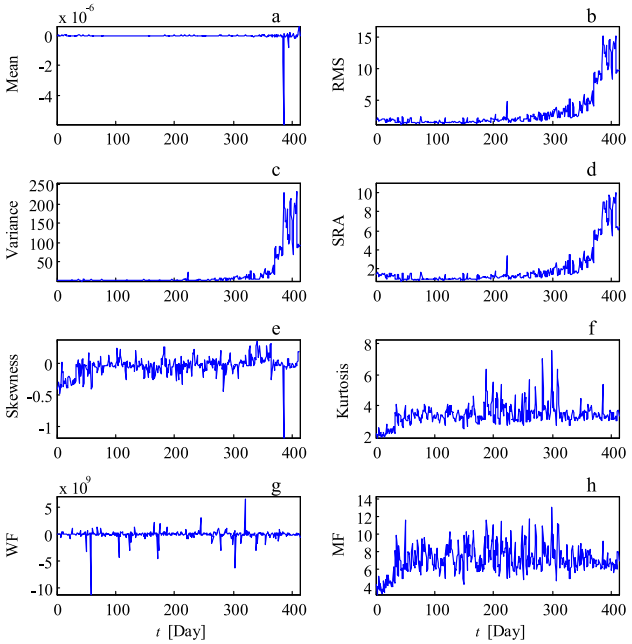

FIGURE 7. Time indicators of bearing 1: a) mean; b) RMS; c) variance; d) square root of amplitude; e) skewness; f) kurtosis; g) waveform factor; h) margin factor.

effective indicators are necessary. Table 4 lists eight statistical indicators of vibration signals.

The eight indicators of bearing 1 are shown in Fig. 7. Apparently, the root mean square in Fig. 7b, variance in Fig. 7c, and square root of amplitude in Fig. 7d possess good monotonicity and tendency, which should be selected as the health indicators of RUL prognosis. With the following issues being considered, RMS is utilized as the health indicator in this paper: (1) RMS is an effective statistical metric, which has explicit threshold in the vibration criteria VDI 3834 [25] that can denote the health state of wind turbines bearings. (2) Although RMS could be influenced by varying operational conditions, the vibration signals with the rotational speed over 1000 rpm of high-speed shafts were collected

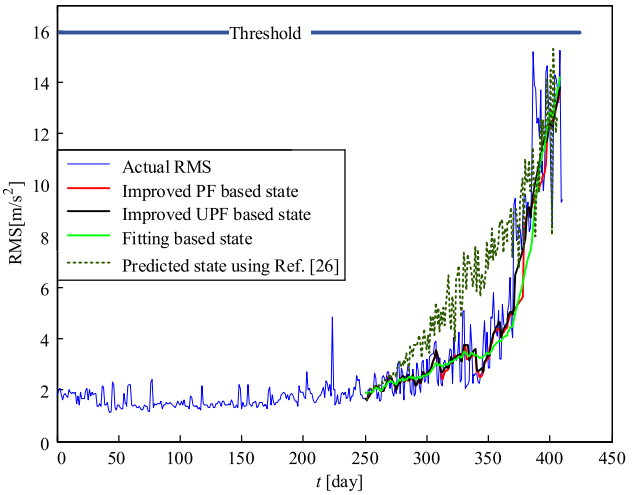

FIGURE 8. RMS of vibration signal of bearing 1, and predicted state with different approaches.

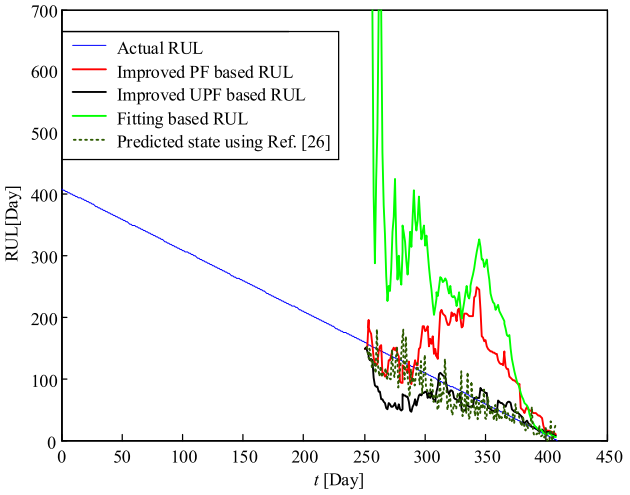

FIGURE 9. Predicted remaining useful life using different approaches for bearing 1.

each day. (3) The proposed method, improved unscented particle filter, enables the estimation of the real value of health indicators, with some noise. The fluctuation in RMS caused by operating conditions can be treated as state noise. (4) In the on-site scenarios, RMS exhibits favorable tendency when the health state of bearings in wind turbines are deteriorating. This is verified not only by the three study cases in this paper, but the published paper, such as [28]. For the high-speed bearings in wind turbines, the failure threshold of RMS is 16 m/s^2.

C. THE RESULTS OF RUL PROGNOSIS

The blue line in Fig. 8 shows the RMS of bearing 1. Although the maximum of RMS didn't exceed the threshold 16 m/s^2, this bearing indeed was replaced after the 413th day. Therefore, the day with maximum RMS is defined as the failure day. In this case, the failure day is the 409th day. Three approaches including improved PF, improved UPF and state fitting are utilized to predict the remaining useful life of the bearing. The improved UPF (our proposed method) obeys the procedure of Table 2, and the improved PF is similar but lacks the unscented transform of Eqs. (12) and (13). State fitting approach adopts single exponential model to fit the data from the $(k\text{-}N)^{th}$ to k^{th}step to get a model parameter. The day with the coming state knocking the threshold under this parameter will be used to calculate the RUL. The fitted result at the k^{th} step is drawn in Fig. 8 as the green line. The predicted state based on improved PF and UPF are shown as the red and black line.

In Section III. B, the initial parameter b is mentioned that it is significant for the prediction of the RUL. As the analysis of abundant on-site bearings on wind turbine high-speed shafts, b is initially set [0.01, 0.02]. The predicted RULs of bearing 1 are shown in Fig. 9. At the early prediction stage, the RULs using three approaches deviate from the true RUL, however,

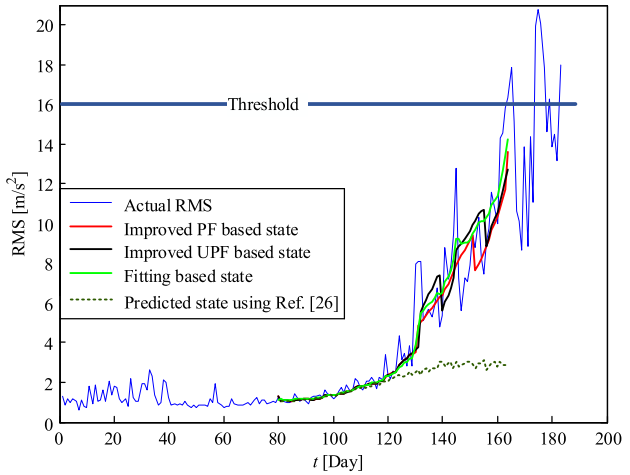

FIGURE 10. RMS of vibration signal of bearing 2, and predicted state with different approaches.

they are gradually close to the true RUL with the bearing being in degradation progress. In Fig. 9, the improved UPF performs superiorly than the other two methods, showing that the proposed approach can adjust its prognosis result by the arriving measurements, rather than the initial parameter. This demonstrates that the proposed approach is practicable in the bearing RUL prognosis of wind turbine high-speed shafts.

The RMS of bearing 2 in Fig. 10 exhibits intensive fluctuation during its life cycle, which accords to the characteristic of varying rotational speed and load of wind turbines. Nevertheless, the three approaches (improved UPF, improved PF, and state fitting) can still handle the fluctuating health indicator, and get the tracking states, which are shown as the black, red and green line separately. The failure day in this case is the time knocking the threshold, the 165th day. The initial parameter b is sampled in the same range [0.01, 0.02]. The predicted RULs in Fig. 11 are gradually close to

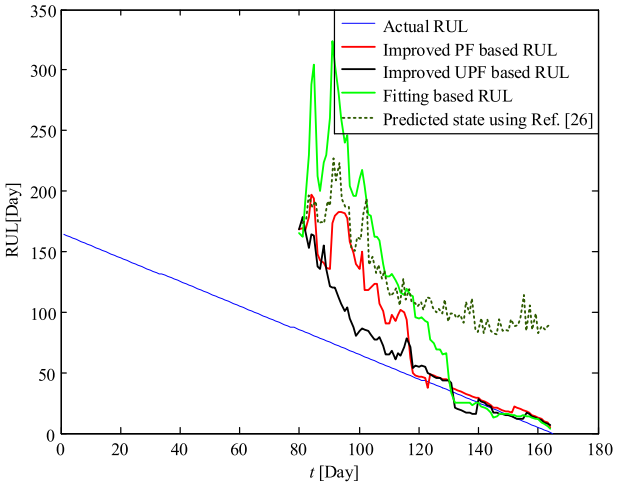

FIGURE 11. Predicted remaining useful life using different approaches for bearing 2.

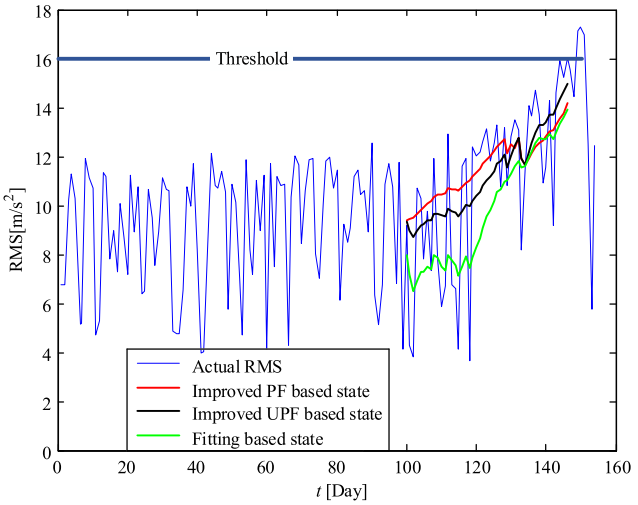

FIGURE 12. RMS of vibration signal of bearing 3, and predicted state with different approaches.

the true RUL, amongst these, the improved UPF based approach performs better than the other methods before the 130$^{\text{th}}$ day and the state fitting is superior after the 130$^{\text{th}}$ day.

The RMS of bearing 3 shows some differences to the two bearings ahead. Even though it is in good health stage during the first 100 days, the vibration amplitudes are larger, which might be caused by the drawbacks in original manufacturing and installation. The RUL prediction is triggered when the RMS starts an ascending trend and the tracking states are shown in Fig. 12 using the three different approaches. The initial parameter b is sampled from the range [0.01, 0.02] as well. In the RUL results of Fig. 13, the improved UPF shows a more distinct advantage than the other two approaches, because it is more close to the true RUL.

To evaluate the RUL prognosis effect of different approaches, the mean absolute deviation (MAD),

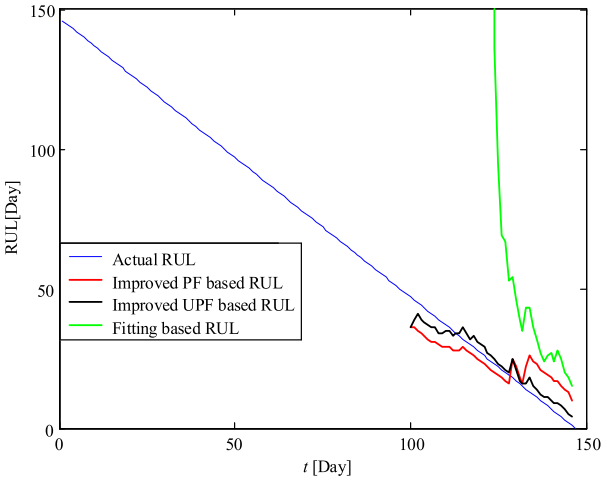

FIGURE 13. Predicted remaining useful life using different approaches for bearing 3.

TABLE 5. MAD of the RUL prediction results of the three bearings (unit: days).

	Total days	Improved UPF	Improved PF	State fitting
Bearing 1	From the 250$^{\text{th}}$ to 408$^{\text{th}}$ day, K=159	**26.73**	58.15	173.3
Bearing 2	From the 80$^{\text{th}}$ to 164$^{\text{th}}$ day, K=85	**20.08**	34.58	65.28
Bearing 3	From the 100$^{\text{th}}$ to 146$^{\text{th}}$ day, K=47	**3.19**	7.27	436.7
Bearing 1	The last 30 days, K=30	**5.19**	22.74	16.13
Bearing 2	The last 30 days, K=30	**5.29**	5.87	3.67
Bearing 3	The last 30 days, K=30	**3.77**	6.61	249.4

$\sum_{k=1}^{K} |\text{RUL}_k - \text{RUL}_{ak}|/K$, is calculated as Table 5. RUL_k is the predicted remaining useful life using three different approaches, RUL_{ak} is the actual remaining useful life at the k^{th} step. K is the total prognosis step.

In Table 5, the improved UPF based approach has a higher prediction accuracy than the other two methods when starting the RUL prognosis procedure at the incipient fault stage of the three bearings. For the last 30 days, a critical period when maintenance strategy is scheduled, the MAD of the improved UPF is only 5 days around, which can assist to provide an accurate failure time for operation and maintenance at wind farms.

D. COMPARISON WITH OTHER RUL PROGNOSIS METHOD

Many particle filter based methods were developed for RUL prognosis. For example, in reference [26], the authors proposed a tutorial for particle filter based prognostics algorithm that can be used in the prognosis of battery degradation and crack growth. This method is adopted to predict the RULs of the bearings in this paper. The same range [0.01, 0.02] for b is used. In the predicted result of bearing 1 in Fig. 8,

the predicted state (dash line) corresponds to the measured RMS. The predicted RUL in Fig. 9 fluctuates around the true RUL, exhibiting a feasible prognosis result of RUL.

The same method and parameters are used for the prediction of bearing 2, and the result is shown in Fig. 10. The predicted state (dash line) in Fig. 10 deviates from the measured RMS gradually with the deterioration of bearing 2. Consequently, the predicted RUL in Fig. 11 is far from the true RUL, which cannot provide practical maintenance suggestion at wind farms.

As a comparison, from the results in Figs. 9, 11 and 13, the proposed improved UPF approach provides accurate RUL results for the three bearings, which demonstrates that the proposed approach is robust, and insensitive to the initial model parameter. Through the proposed resampling technique, model parameter b is updated with the selected large weight particles and the arriving measurements, thus showing a superior adaptability.

V. CONCLUSION

Bearings remaining useful life prognosis plays a significant role in the operation and maintenance of wind turbines. However, varying speed and load, inappropriate model parameters may block the successful application of remaining useful life prognosis in on-site wind turbines.

In this paper, a robust model-based approach with improved unscented particle filter is proposed, involving three aspects: (1) Replacing the particles using the mean from unscented Kalman transform to enhance particle aggregation; (2) Using past measurements to estimate the variance in likelihood calculation; (3) A resampling technique is presented to guarantee the particle diversity. Based on the improvements, the procedure of bearing remaining useful life prognosis in wind turbines is presented and verified by three life-cycle bearings from on-site wind turbines. The results illustrate that the proposed approach can accurately predict the remaining useful life of bearings, which will provide feasible maintenance suggestions for wind farms.

REFERENCES

[1] *Wind Power Capacity Worldwide Reaches 597 GW, 50,1 GW Added in 2018*. Accessed: Jun. 4, 2019. [Online]. Available: https://wwindea.org/blog/2019/02/25/wind-power-capacity-worldwide-reaches-600-gw-539-gw-added-in-2018/

[2] J. Z. Sikorska, M. Hodkiewicz, and L. Ma, "Prognostic modelling options for remaining useful life estimation by industry," *Mech. Syst. Signal Process.*, vol. 25, no. 5, pp. 1803–1836, Jul. 2011.

[3] P. Paris and F. Erdogan, "A critical analysis of crack propagation laws," *J. Basic Eng.*, vol. 85, no. 4, pp. 528–533, Dec. 1963.

[4] D. An and J.-H. Choi, "Improved MCMC method for parameter estimation based on marginal probability density function," *J. Mech. Sci. Technol.*, vol. 27, no. 6, pp. 1771–1779, Jul. 2013.

[5] D. Pan, J.-B. Liu, and J. Cao, "Remaining useful life estimation using an inverse Gaussian degradation model," *Neurocomputing*, vol. 185, pp. 64–72, Apr. 2016.

[6] M. S. Arulampalam, S. Maskell, N. Gordon, and T. Clapp, "A tutorial on particle filters for online nonlinear/non-Gaussian Bayesian tracking," *IEEE Trans. Signal Process.*, vol. 50, no. 2, pp. 174–188, 2002.

[7] C. Chang and R. Ansari, "Kernel particle filter for visual tracking," *IEEE Signal Process. Lett.*, vol. 12, no. 3, pp. 242–245, Mar. 2005.

[8] K. Nummiaro, E. Koller-Meier, and L. V. Gool, "Object tracking with an adaptive color-based particle filter," in *Proc. Joint Pattern Recognit. Symp.*, in Lecture Notes in Computer Science, 2002, pp. 353–360.

[9] R. Faragher, "Understanding the basis of the Kalman filter via a simple and intuitive derivation [Lecture Notes]," *IEEE Signal Process. Mag.*, vol. 29, no. 5, pp. 128–132, Sep. 2012.

[10] Y. Lei, N. Li, S. Gontarz, J. Lin, S. Radkowski, and J. Dybala, "A model-based method for remaining useful life prediction of machinery," *IEEE Trans. Rel.*, vol. 65, no. 3, pp. 1314–1326, Sep. 2016.

[11] E. Zio and G. Peloni, "Particle filtering prognostic estimation of the remaining useful life of nonlinear components," *Rel. Eng. Syst. Saf.*, vol. 96, no. 3, pp. 403–409, Mar. 2011.

[12] C. Chen, G. Vachtsevanos, and M. E. Orchard, "Machine remaining useful life prediction: An integrated adaptive neuro-fuzzy and high-order particle filtering approach," *Mech. Syst. Signal Process.*, vol. 28, pp. 597–607, Apr. 2012.

[13] J. Fan, K.-C. Yung, and M. Pecht, "Predicting long-term lumen maintenance life of LED light sources using a particle filter-based prognostic approach," *Expert Syst. Appl.*, vol. 42, no. 5, pp. 2411–2420, Apr. 2015.

[14] N. Raghavan and D. D. Frey, "Particle filter approach to lifetime prediction for microelectronic devices and systems with multiple failure mechanisms," *Microelectron. Rel.*, vol. 55, nos. 9–10, pp. 1297–1301, Aug. 2015.

[15] M. E. Orchard and G. J. Vachtsevanos, "A particle filtering-based framework for real-time fault diagnosis and failure prognosis in a turbine engine," in *Proc. IEEE Medit. Conf. Control Automat.*, Athens, Greece, Jun. 2007, pp. 1–6.

[16] A. Doucet, N. D. Freitas, and E. Wan, "The unscented particle filter," in *Proc. NIPS*, vol. 13, Aug. 2001, pp. 584–590.

[17] D. E. Acuña and M. E. Orchard, "Particle-filtering-based failure prognosis via sigma-points: Application to lithium-ion battery State-of-Charge monitoring," *Mech. Syst. Signal Process.*, vol. 85, pp. 827–848, Feb. 2017.

[18] X. Zheng and H. Fang, "An integrated unscented Kalman filter and relevance vector regression approach for lithium-ion battery remaining useful life and short-term capacity prediction," *Rel. Eng. Syst. Saf.*, vol. 144, pp. 74–82, Dec. 2015.

[19] H. Qiu, J. Lee, J. Lin, and G. Yu, "Robust performance degradation assessment methods for enhanced rolling element bearing prognostics," *Adv. Eng. Informat.*, vol. 17, nos. 3–4, pp. 127–140, Jul. 2003.

[20] J. Yu, "A hybrid feature selection scheme and self-organizing map model for machine health assessment," *Appl. Soft Comput.*, vol. 11, no. 5, pp. 4041–4054, Jul. 2011.

[21] S. Hong, Z. Zhou, E. Zio, and W. Wang, "An adaptive method for health trend prediction of rotating bearings," *Digit. Signal Process.*, vol. 35, pp. 117–123, Dec. 2014.

[22] W. Teng, X. Zhang, Y. Liu, A. Kusiak, and Z. Ma, "Prognosis of the remaining useful life of bearings in a wind turbine gearbox," *Energies*, vol. 10, no. 1, p. 32, Dec. 2016.

[23] L. Guo, N. Li, F. Jia, Y. Lei, and J. Lin, "A recurrent neural network based health indicator for remaining useful life prediction of bearings," *Neurocomputing*, vol. 240, pp. 98–109, May 2017.

[24] J. D. Hol, T. B. Schon, and F. Gustafsson, "On resampling algorithms for particle filters," in *Proc. Nonlinear Stat. Signal Process. Workshop*, Cambridge, U.K., Sep. 2006.

[25] *Measurement and Evaluation of the Mechanical Vibration of Wind Energy Turbines and Their Components Onshore Wind Energy Turbines With Gears*, document VDI 3834, 2009, p. 16.

[26] D. An, J.-H. Choi, and N. H. Kim, "Prognostics 101: A tutorial for particle filter-based prognostics algorithm using MATLAB," *Rel. Eng. Syst. Saf.*, vol. 115, pp. 161–169, Jul. 2013.

[27] J. Deutsch, M. He, and D. He, "Remaining useful life prediction of hybrid ceramic bearings using an integrated deep learning and particle filter approach," *Appl. Sci.*, vol. 7, no. 7, p. 649, Jun. 2017.

[28] F. Cheng, L. Qu, W. Qiao, and L. Hao, "Enhanced particle filtering for bearing remaining useful life prediction of wind turbine drivetrain gearboxes," *IEEE Trans. Ind. Electron.*, vol. 66, no. 6, pp. 4738–4748, Jun. 2019.

[29] F. Cheng, L. Qu, and W. Qiao, "Fault prognosis and remaining useful life prediction of wind turbine gearboxes using current signal analysis," *IEEE Trans. Sustain. Energy*, vol. 9, no. 1, pp. 157–167, Jan. 2018.

[30] M. A. Djeziri, S. Benmoussa, and R. Sanchez, "Hybrid method for remaining useful life prediction in wind turbine systems," *Renew. Energy*, vol. 116, pp. 173–187, Feb. 2018.

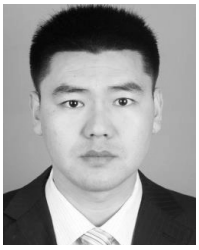

WEI TENG received the B.S. degree in mechanical engineering from the University of Science and Technology, Beijing, China, in 2004, and the Ph.D. degree in mechanical engineering from the Huazhong University of Science and Technology, Wuhan, China, in 2009.

He is currently an Associate Professor with the School of Energy Power and Mechanical Engineering, North China Electric Power University, Beijing. His current research interests include fault diagnosis and failure prognostic, data mining, predictive maintenance, and their applications to mechanical systems in energy and power field.

CHEN HAN received the B.S. degree in mechanical engineering and automation from North China Electric Power University, Beijing, China, in 2016, and the M.S. degree in mechanical engineering, in 2019. He is currently pursuing the Ph.D. degree with the School of Mechanical Engineering, Zhejiang University, Hangzhou.

YANKANG HU received the B.S. degree in industrial engineering from the Nanjing Institute of Technology, Nanjing, China, in 2018. He is currently pursuing the master's degree with the School of Energy Power and Mechanical Engineering, North China Electric Power University, Beijing. His current research interests are mechanical and electrical control.

XIN CHENG received the B.S. degree in information engineering and the M.S. degree in communication and information system from the Wuhan University of Technology, Wuhan, China, in 2004 and 2007, respectively, and the Ph.D. degree in mechanical and electronic engineering from the Huazhong University of Technology, Wuhan, in 2011.

He is currently an Associate Professor with the School of Mechanical and Electronic Engineering, Wuhan University of Technology. His research interests include motion control, fault-diagnosis and fault-tolerant control, magnetic bearings, and advanced servo systems.

LEI SONG received the Ph.D. degree in thermal energy engineering from North China Electric Power University, Beijing, China, in 2015.

He is currently an Assistant Researcher with the Data Analysis Group, Payload Operation and Control Center, Technology and Engineering Center for Space Utilization, Chinese Academy of Sciences, Beijing. His current research interests include failure analysis, anomaly detection, condition monitoring, health management, and their application to mechanical system in aerospace and energy engineering.

YIBING LIU received the B.S. degree in machinery design and manufacture from North China Electric Power University, Baoding, China, in 1982, and the Ph.D. degree in machine manufacturing from University of Hanover, Germany, in 1999.

He is currently a Professor and a Ph.D. Supervisor with the School of Energy Power and Mechanical Engineering, North China Electric Power University, Beijing. His current research interests include fault diagnosis and failure prognostic, reliability centered maintenance, rotor dynamics, predictive maintenance, and their applications to mechanical systems in energy and power field.